Talanta 87 (2011) 197–209

Contents lists available at SciVerse ScienceDirect

Talanta

journal homepage: www.elsevier.com/locate/talanta

Chemometric tools to evaluate the spatial distribution of trace metals in surface sediments of two Spanish rías

Cristina Quelle[a], Victoria Besada[a], José Manuel Andrade[b,*], Noemí Gutiérrez[b], Fernando Schultze[a], Jesús Gago[a,c], Juan José González[a]

[a] Centro Oceanográfico de Vigo, IEO (Instituto Español de Oceanografía), Subida a Radio Faro 50, 36390, Vigo, Spain
[b] Department of Analytical Chemistry, University of Corunna, Campus da Zapateira, E-15008, Corunna, Spain
[c] European Commission – DG ENV, Marine Environment & Water Industry, Avenue de Beaulieu 5, BU 9 – 3/121, 1160 Brussels, Belgium

ARTICLE INFO

Article history:
Received 2 August 2011
Received in revised form
21 September 2011
Accepted 27 September 2011
Available online 1 October 2011

Keywords:
Ría
Trace metals
Sediments
Classification trees
Self-organizing maps
Procrustes rotation

ABSTRACT

A suite of relevant trace metals (Hg, Pb, Cd, Cu, Zn and Ni) was measured in surface sediment samples to assess the environmental situation of the largest two Atlantic Spanish 'rías' (a form of estuaries, ría of Pontevedra, ROP, and ría of Vigo, ROV). The level of contamination originated by these metals was assessed against international guidelines, the threshold effect, ERL, and the midrange effect, ERM. Six unsupervised and supervised multivariate chemometric techniques were applied to model each ría, compare them and select those metals that characterize the samples. This is first time that such a study is performed for these two important seafood-producing areas. Maximum concentrations at ROP occurred in the vicinities of an inner island, where Cu, Zn, Ni and Pb presented concentrations over the ERL and Hg over the ERM. Highest concentrations of metals in ROV were observed in the proximities of Vigo shipyards and port, except for Pb, with peak values in San Simon Bay. ERL limits were exceeded in the inner part of this ría for Cu, Zn and Hg and in a wider area for Pb and Ni. Levels for Pb went beyond the ERM boundary in the axial part of San Simon Bay. In general, the distribution of the metals was more homogeneous in ría of Pontevedra than in ría of Vigo (where three morphological zones were characterized). Both rías could be differentiated using only two metals: Ni and Hg, as deduced from the multivariate techniques.

1. Introduction

Despite metals occur naturally in the Earth's crust, the steady increase on their concentrations in estuaries and coastal zones and, so, in marine organisms, is caused mainly by anthropogenic inputs [1]. As they do not biodegrade, they accumulate in the environment linked to the surface of suspended particles, both organic and inorganic [2,3] Some, like Fe, Cu, Zn and Mn, are essential for organisms, but may become toxic when certain concentrations are exceeded [4]. Others (e.g., Hg, Pb, Cd, As and Cr) are not required for metabolic functions and are toxic even at very low concentrations. A serious consequence of their persistence is their accumulation through the food chain.

It is worth noting that pollutants accumulate in sediments in different ways, depending on their morphologic and geochemical characteristics. In general, the concentrations of metals increase as particle size decreases [2]. This leads to a general accumulation of metals in seabed sediments close to industrial and urban zones, mainly in areas of low hydrodynamic energy. However, they do not remain linked permanently to sediments, as they can be released to the water column and become available for the marine biota [5].

To assist regulators numerous sediment quality guidelines (SQGs) were developed. Traditionally, pollution was determined by assessing the bulk chemical concentrations of individual compounds and comparing them with background or reference values. Since the 1980s, SQGs attempted to incorporate biological effects [6]. Nowadays, some SQGs for metals are used worldwide to identify a level of pollution that may have adverse effects in living organisms [7,8]. In this paper, the approach of Long et al. [9] was adopted. They identified nine metals that had ecological or biological effects on organisms and defined two indexes: the 'Effects Range Low', ERL (the lowest concentration of a metal for which at least 10% of the data reviewed reported adverse effects), and the 'Effects Range Median', ERM (the level at which half of the studies reported harmful effects). Metal concentrations below the ERL are not expected to elicit adverse effects, while levels above the ERM are likely to be very toxic. These SQGs were adopted by the

* Corresponding author. Fax: +34 981 167065.
E-mail address: andrade@udc.es (J.M. Andrade).

0039-9140/$ – see front matter © 2011 Elsevier B.V. All rights reserved.
doi:10.1016/j.talanta.2011.09.062

National Oceanic Atmospheric Administration (NOAA) and other environmental agencies for the assessment of marine pollution in coastal areas.

General rules for metal accumulation also apply to the '*rías*' (a form of estuaries, similar to the Nordic fiords) but they have a more complex behaviour because of their chemical conditions resulting from the mixture of oceanic and continental waters discharged from rivers. This singularity promotes the accumulation of continental contaminants in addition to the oceanic ones [10,11]. Thus, assessing pollution in Galician rías is a quite difficult, although important, issue because of the numerous fish and seafood farming activities performed within them. As an example, Galicia is the first European producer of cultured mussels, with an annual production of 250,000 tons (135×10^6 Euros) [12] and shellfish production in Galicia ranks first in Spain, with more than 10% of the total production [13].

The Spanish Monitoring Programme on wild mussels and sediments was deployed to evaluate the spatial and temporal distribution of hazardous substances and to identify potential pollution sources [14,15]. Nevertheless, it is too focused on some particular objectives, it comprehends hundreds of nautical miles and, accordingly, the number of samples in specific areas of interest is limited. Due to this lack of information, additional research is presented in this paper to study some selected trace metals at two economically relevant Spanish rías (worldwide reputed zones for seafood farming and collection): the ría of Pontevedra, ROP, and the ría of Vigo, ROV. Concentration ranges for some metals on these rías have been reported previously associated to anthropogenic activities at the ROP inner-south area [16–18]. Regarding the whole ROV, only some partial studies were found [19–22].

The present work has, therefore, three main objectives. First, to perform a comprehensive study of six trace metals in surface sediments of the two Spanish rías (metals in living organisms will not be considered nor sedimentary organic pollutants). The six metals analysed were those included in current Spanish maritime monitoring programmes. Second, to assess the level of pollution according to the limits of the SQGs mentioned above, as well as to study the relationship between the metals, their possible sources and the hydrodynamics of the rías. Finally, a suite of multivariate chemometric techniques (principal components analysis, Procrustes rotation, hierarchical clustering by heatmaps, classification and regression trees, linear discriminant analysis and self-organizing maps) were applied to model each ría, compare them and select those metals that characterize critically the environmental situation of the samples [23]. This is first time such a study is performed for these two important seafood producing and farming areas. In addition, objective variable selection has scarcely been presented in related literature to schedule future monitoring programmes, despite its inherent savings in overall costs, improved analyses turnaround time, reduction of redundant information (e.g., because of strongly correlated variables), etc.

2. Materials and methods

2.1. Sampling area

The strong influence oceanographic conditions have on the depositional characteristics of particulate matter within the rías requires their brief description here. The term '*ría*' refers to major coastal inlets formed after some river valleys sunk. These geological formations are characteristic of the NW Iberian Peninsula, the rías of Pontevedra (ROP) and Vigo (ROV) being two of the largest ones (42.1–42.45°N, 8.6–8.95°W, Fig. 1). They are located at the Northern most limit of the Eastern North Atlantic Upwelling System, which extends from 10° to about 44°N [24]. A spring–summer process characterized by favorable northerly winds along the coast produces an offshore zonal Ekman transport of surface water. This is replaced by cold nutrient-rich deep water (the Eastern North Atlantic Central Water) [25,26]. During autumn-winter favorable southerly winds are predominant, generating the opposite dynamics and, consequently, downwelling.

The rías are mixed estuaries with a two-layer residual positive circulation [27,28]. This pattern can be modified by the winds over the shelf. These embayments are open systems with a major exchange with oceanic waters so that when shelf winds induce upwelling events, a positive circulation occurs in the rías. On the other hand, during strong downwelling conditions, water from the shelf entering the ría causes the water inside it to be advected to the shelf through lower layers [29].

The ría of Pontevedra is a V-shaped coastal embayment that opens up to the north of Ría de Vigo (its volume and surface are around 3.937 hm^3 and 145 km^2). Its central axis is oriented SW–NE. The depth of the ría decreases to the inner part where sedimentation of mud and sand takes place, especially in the southern margin. The ROP extends 23 km from its head at river Lérez (E) to the Islands of Ons and Onza (W). Its width decreases progressively towards the river Lérez mouth. It has been divided into three morphological zones: the inner (sites 1–7), intermediate (sites 8–12) and outer (sites 13–23) ones (Fig. 1).

The ría of Vigo is the Southern most Spanish one (total volume ca. 3.117 hm^3 and 176.4 km^2 surface). It is a V-shaped formation, with its central axis oriented NE–SW. The water depths range from 7 (inner part) to 53 m (SW exit to the sea). It has been commonly divided into three morphological zones: the inner or estuarine (sites 1–13); intermediate (sites 14–28) and outer or oceanic (sites 29–36) zones, Fig. 1. The maximum width is at the mouth of the embayment (5.2 km) and it diminishes progressively down to 600 m at the Rande strait. The mouth of the ría is partially closed by the Cíes Islands.

2.2. Sampling and sample preparation

A total of 23 and 36 sampling points were considered at ROP and ROV, respectively, Fig. 1. Surface sediment samples (0–5 cm) were collected with a "Box- Corer" grab from the research vessel José María Navaz. Sampling sites were far from sewers that could affect the results. Samples were stored in clean containers and kept at −20 °C till their lyophilization.

An important issue to be considered is the sediment fraction to be analysed, as the concentrations of metals can vary depending on the selected fraction [30]. According to the International Council for the Exploration of the Sea (ICES), the analyses were carried out on the fraction below 2 mm ('total fraction'). Following, freeze-dried samples were sieved through a 2 mm mesh, homogenized and stored in acid-washed glass vials at room temperature until chemical analysis.

2.3. Chemical analyses

Analysis of Pb, Cd, Cu, Zn and Ni included total digestion in a CEM MARSXpress microwave oven. 0.3 g of freeze-dried sample were placed in a Teflon reactor, with 1 ml of aqua-regia and 5 ml of Hydrofluoric acid. The reactor was kept at 160 °C for 30 min. Then, 4.7 g of boric acid were added and the volume was adjusted to 50 ml with Milli-Q water (more details can be found elsewhere [31]). An AAnalyst 800 PerkinElmer spectrophotometer (Zeeman background correction) was used, along with the operational parameters and matrix modifiers recommended by the manufacturer.

Nitric digestion was applied for total Hg analysis; 0.5 g of sample and 5 ml of concentrated nitric acid were digested at 160 °C for

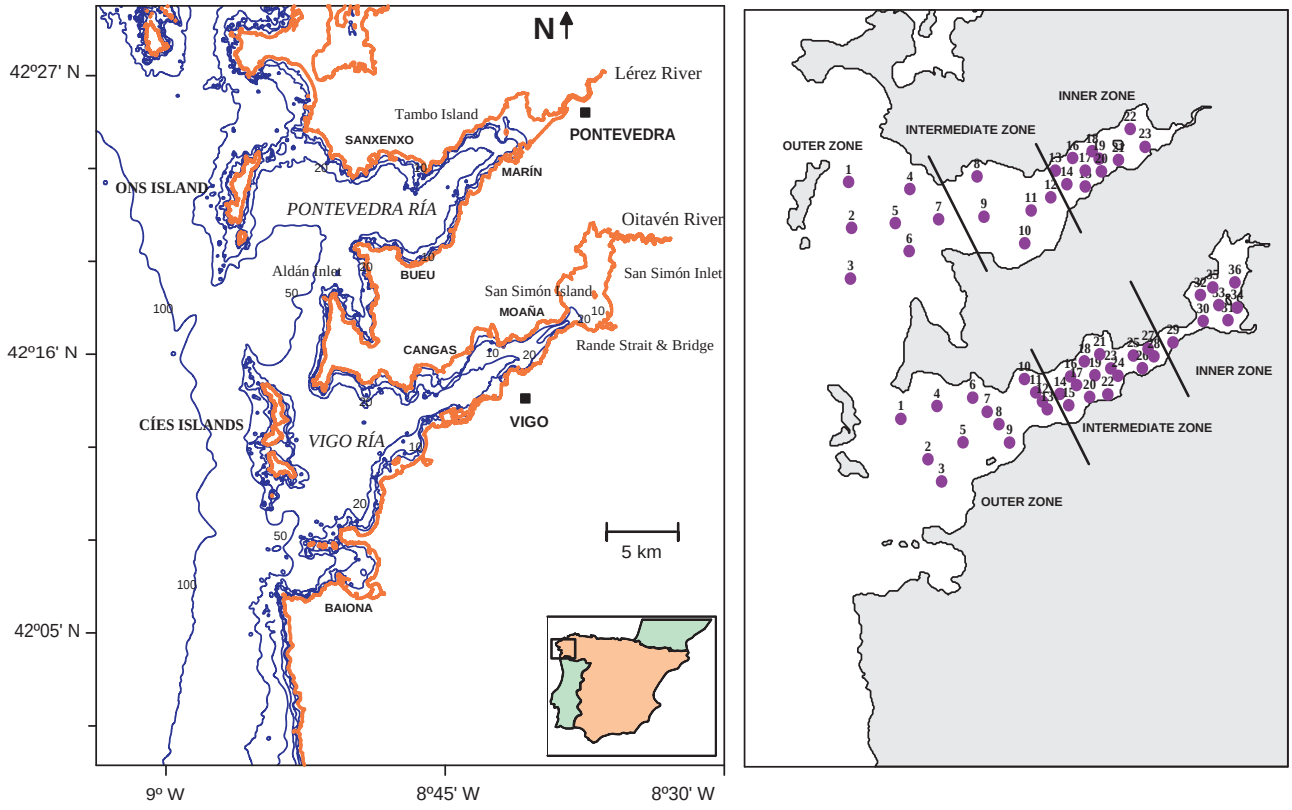

Fig. 1. Map of the ría of Pontevedra and ría of Vigo, Galicia, NW of Spain. Location of sampling sites and main morphological zones at both 'rías'.

30 min in a microwave oven. The cold vapour technique was applied on a FIMS-400 PerkinElmer system, with a reducing solution of 10% $SnCl_2$ in 6% (v/v) HCl. The detection limits expressed in mg kg^{-1} dry weight were: 0.005 for Hg, 1.00 for Pb; 0.008 for Cd, 0.500 for Cu, 2.00 for Zn and 1.00 for Ni.

The total organic carbon (TOC) in sediments was measured by oxidation with potassium dichromate in a strongly acidic medium, followed by titration of the ferrous ammonium sulphate from the surplus dichromate remaining after oxidation [32]. The fraction below 63 μm was also determined by wet sieving and subsequent drying and weighing of the sieved fraction, in order to characterize the sediment and facilitate data assessment.

The analytical procedures were validated by a quality assurance system. Protocols incorporated the use of certified reference materials (BCSS-1 and BEST-1, National Research Council of Canada), duplicate samples, procedural blanks and control charts, as well as participation in international intercomparison exercises, such as QUASIMEME (Quality Assurance of Information in Marine Environmental Monitoring in Europe). The analytical results (mean ± SD) of six independent analyses are shown in Table 1 and agreed with the certified values. In addition, recovery studies spiking aliquots of the reference materials, yielded average recoveries between 96% (Hg) and 104% (Cd).

Table 1
Comparison between experimental results and certified values for certified reference material (BCSS-1). Values are given in mg kg^{-1} dry weight.

Element	Certified	Measured
Mercury[a]	0.092 ± 0.009	0.088 ± 0.002
Lead	22.7 ± 3.4	23.3 ± 2.2
Cadmium	0.25 ± 0.04	0.26 ± 0.03
Copper	18.5 ± 2.7	19.1 ± 1.3
Zinc	119 ± 12	112 ± 4
Nickel	55.3 ± 3.6	53.1 ± 3.2

[a] CRM used, BEST-1.

2.4. Software

The statistical studies were made using GenEx (MultiD Analyses AB, Sweden), Statgraphics (StatPoint Technologies Inc, US), Jatoon (Java Tools for Neural Networks, www.dq.fct.unl.pt/staff/jas) and CART (http://cran.r-project.org/, RPART library; v2.4.0).

3. Results and discussion

3.1. Univariate studies

A preliminar univariate study was performed considering all samples. Metal values are reported as mg kg^{-1} in Tables 2 and 3. The number of significant figures of the analytical results of this work corresponded to the criteria stated by QUASIMEME interlaboratory exercises, except for Table 1, which are those reported at the CRMs documentation. TOC and % of fine particles are usually reported with two decimal places. The percentages of sampling sites exceeding ERLs and ERMs in ROP and ROV are also displayed.

ROP surface sediments were a combination of sand and mud. Characterization of the fraction below 63 μm indicated that 47.8% of the samples were constituted mainly by fine particles (Fig. 2a), most of them located at the inner zone of the ría (surroundings of Tambo Island) and in the 'shadow' zone of Ons Islands, where the lower hydrodynamic energy allows sedimentation of fine particles. Some sediments adjacent to Tambo Island showed fine particles over 90%. Sandy samples were mostly located at the outer zone, in areas exposed to the oceanic hydrodynamics, where fine sediments are washed out towards more protected areas. These results were consistent with other studies carried out for this ría [33]. Concentrations of TOC ranged from 0.22% to 6.78%; with higher values at

Table 2
Summary of the concentrations of trace metals (mg kg^{-1} dry weight), percentage of fine particles (grain size <63 μm) and total organic carbon (TOC) in surface sediments of ría of Pontevedra (SD: standard deviation).

	Ría of Pontevedra							
	Mean	Median	Range	SD	ERL	ERM	% Sites over ERL	% Sites over ERM
Hg	0.520	0.130	0.006–1.93	0.681	0.15	0.71	43.5	26.1
Pb	50.4	41.1	13.8–145	30.0	46.7	218	34.8	–
Cd	0.376	0.198	0.058–1.34	0.378	1.2	9.6	4.3	–
Cu	24.9	17.8	3.09–88.8	21.5	34	270	26.1	–
Zn	121	122	13.9–227	62.2	150	410	30.4	–
Ni	14.1	12.7	1.00–29.0	9.26	21	52	30.4	–
%Fine particles	50.44	46.14	2.87–93.22	30.69	–	–	–	–
%TOC	2.45	1.62	0.22–6.78	1.97	–	–	–	–

Table 3
Summary of the concentrations of trace metals (mg kg^{-1} dry weight), percentage of fine particles (grain size <63 μm) and total organic carbon (TOC) in surface sediments of ría of Vigo (SD: standard deviation).

	Ría of Vigo							
	Mean	Median	Range	SD	ERL	ERM	% Sites over ERL	% Sites over ERM
Hg	0.249	0.248	0.012–0.656	0.155	0.15	0.71	69.4	–
Pb	115	103	8.72–268	61.95	46.7	218	83.3	5.6
Cd	0.371	0.381	0.035–1.08	0.245	1.2	9.6	–	–
Cu	43.0	41.1	0.883–165	31.1	34	270	61.1	–
Zn	162	163	11.7–348	68.9	150	410	66.7	–
Ni	31.6	34.8	2.00–47.6	11.7	21	52	86.1	–
%Fine particles	77.11	88.10	2.04–97.37	25.33	–	–	–	–
%TOC	3.14	3.36	0.18–6.75	1.44	–	–	–	–

the inner part of the embayment (Fig. 2c), especially at the northern margin. The presence of numerous mussel rafts in the margins and inner part of the ría may have increased the content of organic matter there [34,35].

ROV surface sediments were composed mainly of fine particles except for five sites located at the outermost part of the northern margin, where sediments were sandy (Fig. 2b). A more homogeneous pattern than in ROP was observed as 63.8% of the sites had fine particles over 80%. TOC varied from 0.18% to 6.75% and it increased substantially towards the inner part of the ría (Fig. 2d); besides, TOC was higher in the axial zone of the external part. The maximum concentration of TOC was observed in site 36, located at

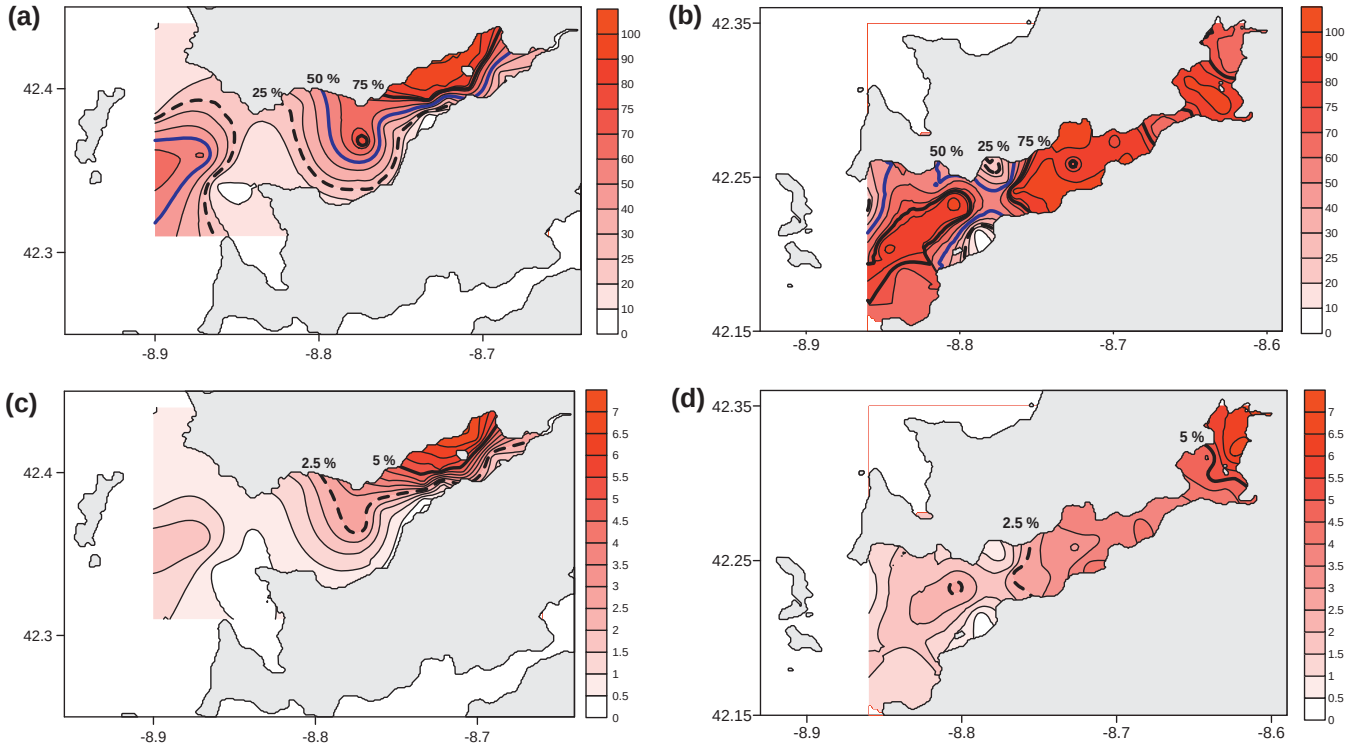

Fig. 2. Percentage of fine fraction (<63 μm) in surface sediment samples of ría of Pontevedra (a) and ría of Vigo (b). Percentage of total organic carbon (TOC) in ría of Pontevedra (c) and ría of Vigo (d).

the inner part of the San Simon Bay. Values of TOC in both embayments were similar to those found in sediments of other estuaries [36].

With regards to the concentration of metals in ROP, some conclusions were drawn. Mercury showed a clear increasing trend towards the inner and northern parts of the ría, probably due to the abundance of fine sediments in these areas (Fig. 3a). Hg varied from 0.006 to 1.93 mg kg^{-1}. The presence of Pb, increased towards the inner part of the ría and to the northern shore (Fig. 3b), although with a wider range of concentrations, from 13.8 to 145 mg kg^{-1}. The trend for Cd was similar to that for Pb (Fig. 3c), with concentrations ranging from 0.058 to 1.34 mg kg^{-1}.

The patterns for Cu and Zn were also similar, with high values in the surroundings of Tambo Island. Their concentrations were in general higher in the northern margin of the ría, decreasing towards its outer and southern parts. Cu ranged from 3.09 to 88.8 mg kg^{-1} in the central zone of the inner part, next to Tambo Island. The northern shore and the axial zone of the embayment protected by the Ons Islands showed higher contents in Zn than the southern margin and the outer part of the ría (Fig. 3e), with concentrations varying from 13.9 to 227 mg kg^{-1}. Ni showed a similar trend, with contents ranging from 1.00 to 29.0 mg kg^{-1}.

As regards ROV, Hg showed an increasing tendency towards the southern margin and the inner part of the ría, and the area adjacent to Vigo city and its harbour (Fig. 3a); it ranged from 0.012 to 0.656 mg kg^{-1}. Pb increased progressively towards the inner part of the southern shore, reaching maximum concentrations in the surroundings of San Simon Island (Fig. 3b). Pb at this ría runs from 8.72 to 268 mg kg^{-1}.

The Cd and Cu distributions followed similar patterns, with maximum concentrations at the central and southern areas of the ría, the area adjacent to Vigo city and port, and at the inner southern shore of San Simon Bay (Fig. 3c and d). Minimum concentrations of Cd and Cu were found in the outer and northern parts of the ría. Cu ranged from 0.883 mg kg^{-1}, at the outermost site, to 165 mg kg^{-1} in the surroundings of some shipyards, while Cd varied from 0.035 to 1.08 mg kg^{-1}. Zn behaved as Cu, Cd and Hg (Fig. 3d).

Ni concentrations presented differences compared to the other metals. It ranged from 2.00 mg kg^{-1}, inner part, to 47.6 mg kg^{-1}, at the intermediate part of the ría, site 22. Values were substantially higher close to Vigo city, although, contrary to other metals, the content of Ni was also significant in the outer zone of the ría (Fig. 3f) probably because of a lithogenic origin, as reported elsewhere [19].

3.2. Comparison with SQGs

Table 2 resumes the main findings for the ría of Pontevedra. Hg was the unique metal for which the ERL (in 43.5% of the sampling sites) and the ERM (26.1% sites) were surpassed. Highest Hg concentrations occur in the surroundings of Tambo Island, where sediments presented concentrations over the ERM, forming a zone of likely toxic effects for half of living organisms (see Fig. 3a). In addition, five other sites exceeded the ERL value. This is probably due to the presence of a nearby industrial complex formed by a chlorine–alkali industry and a paper pulp factory.

Concentrations of Pb surpassed the ERL in 34.8% sampling sites (Fig. 3b), located at the inner part of ROP. The ERL limit for Cd was exceeded only at a site west of Tambo Island (Fig. 3c). Six locations presented values of Cu over the ERL (26.1% of samples), which delimits an area located at the inner and northern part of the embayment (Fig. 3d). Similarly, some locations around Tambo Island presented Zn and Ni values over the ERL (30.4% of sites for both metals; see Fig. 3e and f), although the area where this limit was exceeded was slightly smaller for Ni.

It seemed clear that the area surrounding Tambo Island was the most polluted zone in ROP. Here, Cu, Zn, Ni and Pb exceeded the ERL limits while Hg did so for the ERM limit. Accumulation of metals in this zone might be associated to the former operation of a nearby sewage outfall, now disused. Here, Hg in sediments might produce toxic effects for half of living organisms. This has been previously observed, with concentrations 15 times over the ERM [37]. Most of the northern margin of the ría, (including the northern margin of the central part of the embayment) was also beyond the Hg ERL limit. Metal concentrations found in the present study agree with previous data [18,33] and highlight the presence of local Hg pollution [38].

Table 3 showed that no metals at ROV exceeded the ERM limits, but for Pb at two sites. However, Hg represents a potential hazard since 69.4% of samples exceeded the ERL threshold, most of them from the intermediate and inner parts of the embayment. Many locations overpassed the ERL value established for Pb while sites 33 and 36 surpassed also the ERM limit. They corresponded to the southern shore of San Simón Bay.

Levels of pollution in ROV derived from this study were similar to those reported elsewhere [21,39–41], however values of Pb and Ni are lower than those reported by Howarth et al. [42].

Twenty three sites showed values of Cu over its ERL. With regards to Zn, the ERL was exceeded in most of the intermediate and inner part of the ría, except for sites 35 and 36 placed at the innermost area of San Simon Bay (Fig. 3d), as it was observed for Cu and Ni. As for the latter, 86.1% of sites showed values over the ERL, although the content of Ni in the outer area of the ría, unlike the other metals, was noticeable. No remarkable results were found at ROV for Cd. In general, the distribution pattern of pollution at ROV showed and increasing tendency towards the southern margin and inner part of the ría, as well as the area adjacent to Vigo city and port.

To summarize, ERL limits were exceeded in the inner part of ROV by Cu, Zn and Hg and in most of the ría by Pb and Ni, with maximum concentrations in front of Vigo port, except for Pb.

3.3. Multivariate analyses

In this work, a suite of chemometric techniques was used to unravel the major pollution trends (principal components analysis and self-organizing maps), compare them (Procrustes rotation), study similarities between the samples (hierchical heatmap clustering and classification trees), and look for differences between geographical zones to classify samples (discriminant analysis). They are depicted below and interested readers are encouraged to selected references.

PCA is an unsupervised technique that reduces the dimensionality of the problem, studies correlations between the variables and defines factors which comprise the most relevant information. Besides, very accurate conclusions can be drawn regarding the samples.

Procrustes rotation (PR) determines whether the patterns yielded by several PCA subspaces are similar or not. It is based on the calculation of consensus vectors for each dimensionality. They can be visualized as a sort of 'average' factors calculated between the 1st PCs of the datasets, the 2nd PCs of the datasets and so forth; the closeness of the corresponding PCs of the scores subspaces can be measured by the angle (in degrees) they form. In addition, the consensus vectors can be interpreted in terms of the original variables [43].

Clustering ascertains whether definite groups of samples can be obtained, according to their similarity. The so-called 'heatmap' hierarchical clustering was applied, which is uncommon in the environmental field. The heatmap is a colour-coded two-dimensional mosaic formed by the joint representation of

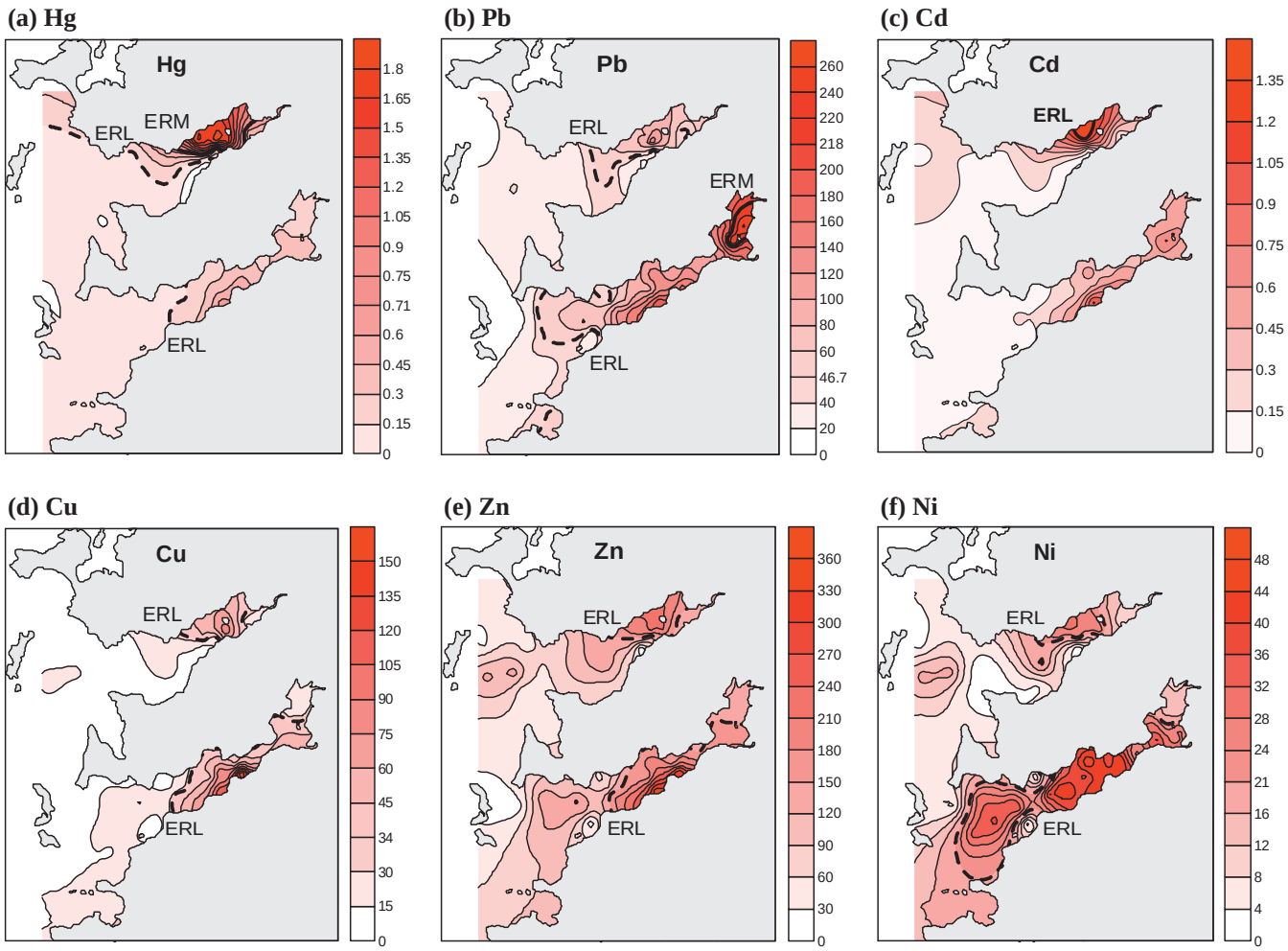

Fig. 3. Isoconcentration maps (mg kg^{-1} dry weight) of trace metals in ría of Vigo and ría of Pontevedra. Distribution of Hg (a), Pb (b), Cd (c), Cu (d), Zn (e) and Ni (f) in surface sediments and location of ERL and ERM boundaries.

two clusters, one is sample-oriented while the other is variable-oriented. Thus, the heatmap describes all similarities within the whole dataset (samples and metals). Note that, as in any typical clustering, the two parameters (similarity and clustering method) need to be selected for each of the two dendrograms. Each tile of the mosaic is coloured with a different intensity according to the values of the (pre-processed) data [44].

'*Classification and regression trees*', CART, is a nonparametric method for classification and regression which aims to find mutually exclusive regions of the data space containing homogeneous subsets of the data [45]. CART can be used to select variables sequentially by means of binary decision trees, containing nodes connected by branches. Nodes giving rise to two new nodes (termed 'child nodes') are called 'parent nodes', otherwise they are 'terminal nodes'. Each node is characterized by a logic rule defined for a single exploratory variable which leads to two child nodes that divide the samples into more homogeneous sets, compared to the original parent node [46].

LDA (linear discriminant analysis) is a supervised classification technique which discriminates the, previously defined, groups of samples by selecting discriminant factors (DFs) that optimally separate the classes [47]. DFs can be interpreted in terms of the experimental variables that determine mostly the combination of variables.

Artificial neural networks based on the unsupervised Kohonen approach (Kohonen maps or self-organizing maps, SOMs) constitute another method to group the samples problems. In SOMs similar input objects are linked to the topologically closest neurons in the network, i.e., neurons that are located close to each other have similar reactions to similar inputs, while the neurons that are far apart have different reactions to similar inputs. The number of neurons and number of epochs to train the SOM must be optimized [48,49].

All multivariate analyses were made on autoscaled data. The samples were codified with a letter (to denote either the ría of Pontevedra, P, or the ría of Vigo, V) and an ordinal number. Preliminary studies revealed that sample P15 behaved as a clear outlier because of its very low concentrations in all metals and total carbon (0.22%). This was attributed to the fact that it had a minute percentage of fine particles (<63 μm), 2.87%, because it was sampled in a site with, essentially, small stones and shells. Therefore, this sample was eliminated from the studies presented hereinafter. Two studies will be presented considering the two rías (ROP and ROV) and the ría of Vigo alone.

3.3.1. *Principal components analysis*

A first PCA was made considering both rías. Three PCs explained 92.86% of the overall variance of the system. The first (67.71% explained variance) was defined mainly by %TOC, Cd, Zn and Cu; which characterized the main distribution of the samples. The 2nd PC (15.02% of the variance) was related to Hg and Ni, which were two relevant metals for ROP and ROV, as explained at the

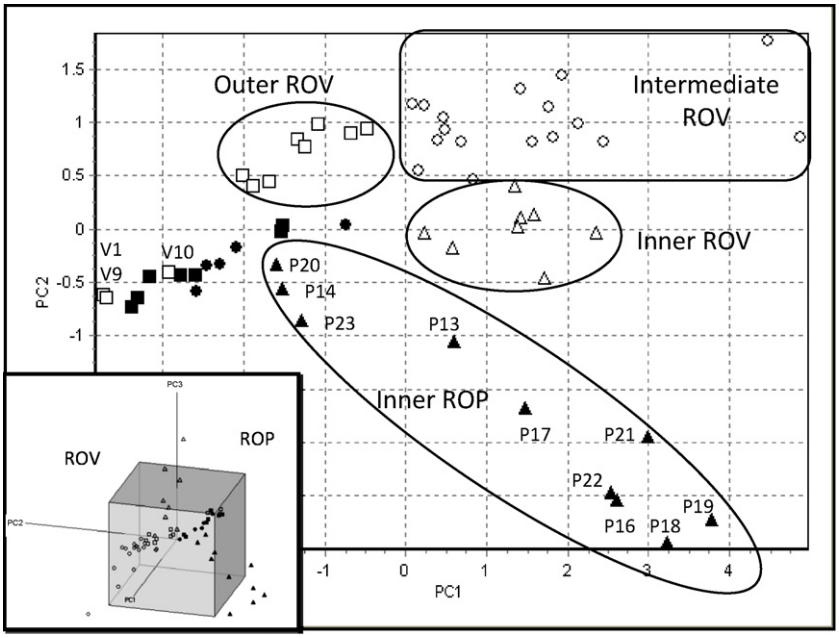

Fig. 4. Scores plot of the PCA considering both rías. The inset shows the PC1–PC2–PC3 subspace. Codes: (■) outer-ROP, (●) intermediate-ROP, (▲) inner-ROP, (□) outer-ROV, (○) intermediate-ROV, (△) inner-ROV.

univariate studies. Finally, the 3rd PC (10.13% of the variance) was linked almost exclusively to Pb at ROV, which suggested a clear relation to anthropogenic sources (as anticipated in Section 3.1).

The PC1–PC2–PC3 scores plot (inset in Fig. 4) revealed that both rías could be differentiated quite easily along PC2 and PC3. The exceptions occurred for samples V1, V9 and V10. They three were from ROV bottom sites containing low amounts of fine sediments and mud (percentages of fine particles between 2% and 19%) and, so, with low concentrations of metals and %TOC. These samples were taken at the outer part of ROV and had metal concentrations of the same order of those from the least polluted samples from the external part of ROP. As mentioned above ROV sediments were composed mainly of fine particles except for sites located at the outermost part, where sediments were mostly sandy.

The PC1–PC2 subspace (Fig. 4) showed a good separation between both rías along PC2 (but for the V1, V9 and V10 samples, just explained) and, furthermore, a nice differentiation between the three zones in which the ROV was divided from a morphological and hydrodynamical point of view (see Section 2.1). Also, the inner zone of ROP became quite clearly characterized by negative scores in PC2, which corresponded both to the highest concentrations of Ni and the overall-samples maxima of Hg. Interestingly, samples P16, P18, P19, P21 and P22 contained the maximum concentrations of Hg (ranging from 1.22 to 1.93 mg kg^{-1}). They located around the small Island of Tambo and had, in general, the highest concentrations of all metals. This agreed totally with the univariate descriptions above and was justified by the depositional behaviour of the ría. Note that these samples corresponded to a ROP area which overpassed the ERM limit for Hg.

Samples from ROV had, in general, higher average values of Ni than the ROP ones. As detailed, Ni levels were substantially higher close to Vigo city, although, contrary to other metals, its contents are also significant in the outer zone of the ría (this may suggest a lithological origin for this metal). PC1 yielded a mere differentiation between the samples with minimum values in most metals, corresponding to the outermost samples of the rías (squares in the figures), remarkably the ROP external ones (Fig. 4).

Fig. 5 presents the PC2–PC3 scores subspace where from an interesting pattern was observed. This consisted of the ordering of the inner samples of ROV as a function of the distance to the bridge of Rande, which belongs to the AP9 highway and supports ca. 70,000 vehicles per day. This might transfer Pb and other metals to the marine environment [22,40]. Fortunately, bans on leaded fuel established in 2001 have cut down such contribution, which would explain the general diminution of Pb concentrations reported elsewhere [50,51]. Despite this, Pb will last on sediments for years. In addition, an old pottery factory was in this area for many years [52] (which used Pb for the varnishes [53,54]) and it released wastes and vitreous materials to the ría. Finally, pollution by Pb might be related also to the intense activity of the port of Vigo and some shipyards.

Fig. 4 showed that the outer and intermediate samples from ROP could not be differentiated. This was so even after a PCA with the ROP samples alone was made. On the contrary, a factor analysis made on the ROV samples demonstrated that the three zones could be observed and, further, that the pattern observed in Fig. 5 for Pb

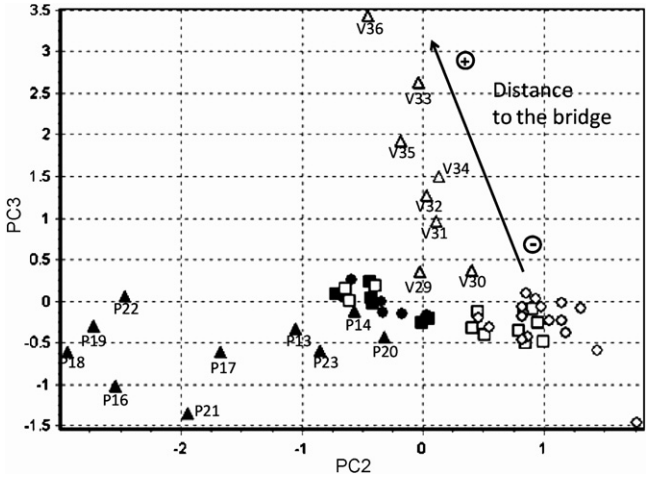

Fig. 5. PC2–PC3 scores subspace of the two rías, showing that ROVI inner samples became affected by Pb. Codes: (■) outer-ROP, (●) intermediate-ROP, (▲) inner-ROP, (□) outer-ROV, (○) intermediate-ROV, (△) inner-ROV.

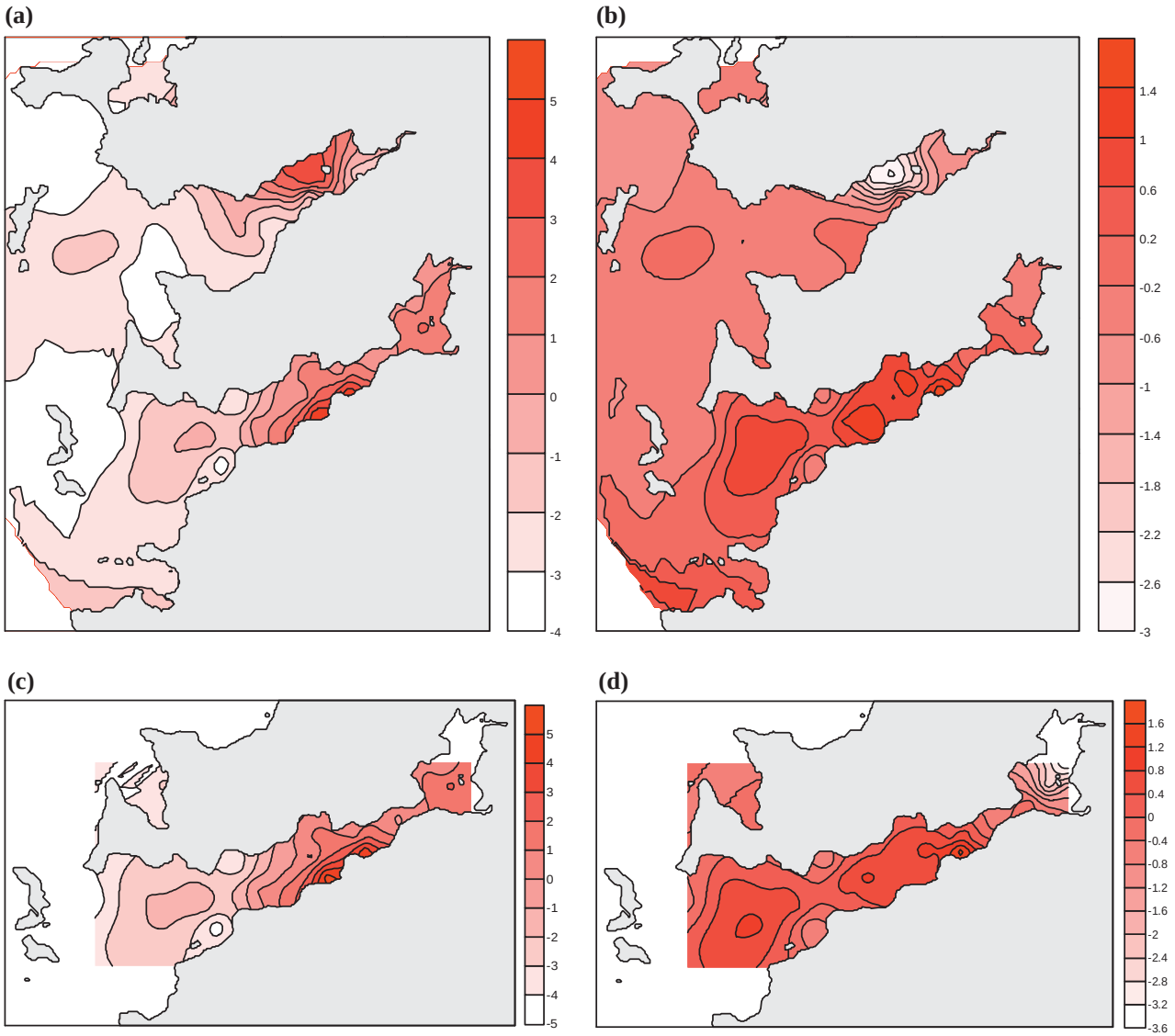

Fig. 6. Iso-scores maps developed for PC1 and PC2 considering both rías (a and b, respectively) and the ría of Vigo (c and d, respectively).

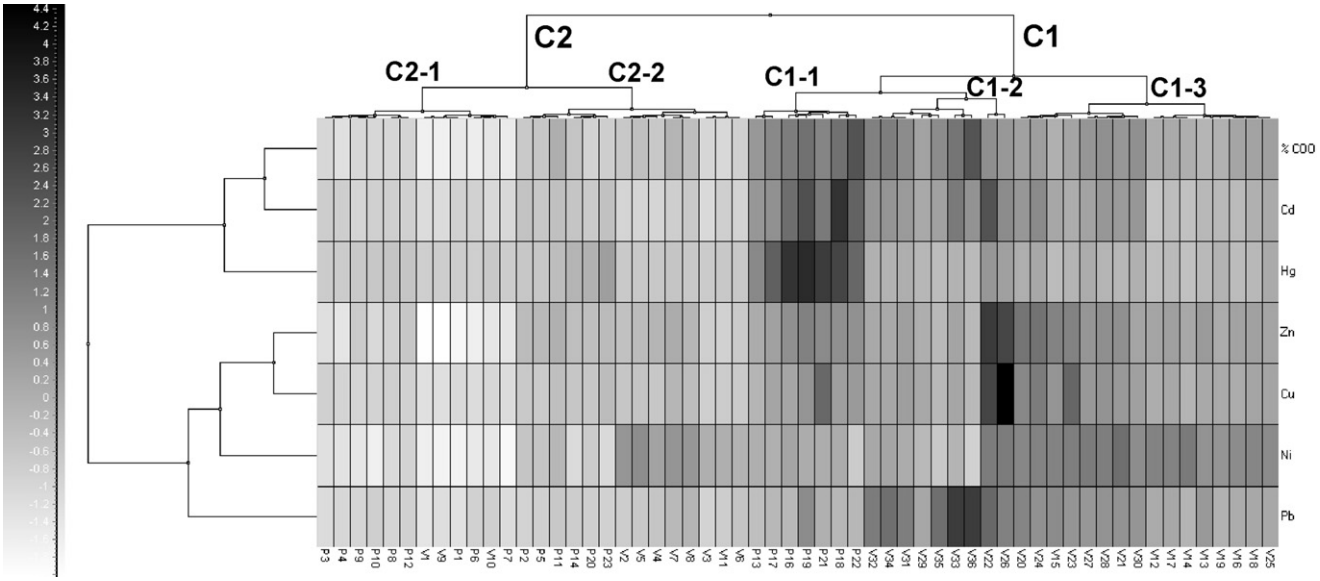

Fig. 7. Heatmap of the overall sample set. P corresponds to ría of Pontevedra and V to the ría of Vigo. The scale at the left represents autoscaled data.

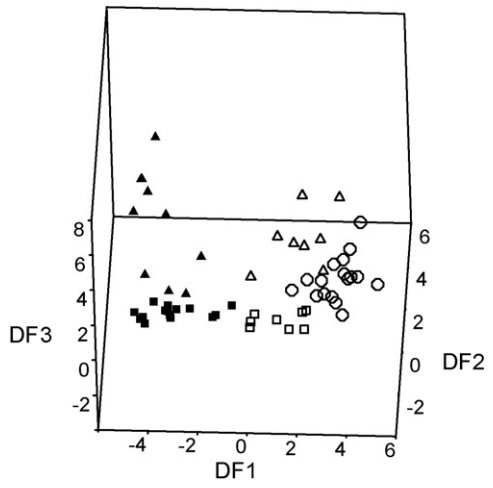

Fig. 8. Representation of the samples at the discriminant DF1-DF2-DF3 space. Codes: (■) outer-ROP, (●) intermediate-ROP, (▲) inner-ROP, (□) outer-ROV, (○) intermediate-ROV, (Δ) inner-ROV.

held. Here, two PCs explained 89.57% of the variance and they were considered enough to describe the ROV. The 1st PC (72.41% of the information) was defined by Cd, Zn and Hg whereas the 2nd was determined by Ni and Pb. As expected, the less polluted samples corresponded to the outer part of the ría, which were defined by negative scores on the 1st PC and values around zero for the 2nd factor. Intermediate samples became characterized by positive scores in both the 1st and 2nd factors. Finally, inner samples had positive scores in PC1 and negative ones in PC2, ordered in accordance to the distance of the bridge of Rande, as explained above. The scores plots for the 1st and 2nd PCs (Fig. 6) looked very much like the geographical patterns of Cd and Zn, and Ni, respectively.

After the PCA studies a decision table was developed (Table 4) considering the metals that defined the two PCs in order to, first, evaluate whether the groups could be differentiated among them and, second, establish decision rules that may allow for a fast classification of unknown samples in future studies. As expected, the rules were affected by the overlap of the groups observed in the PC scores plots. Thus, the outer and intermediate sampling sites of ROP had to be considered altogether in a unique group (along with the V1, V9 and V10 samples from ROV). A 95% success assignation ratio was obtained as only three samples (two outer stations – P2 and P5 – and an intermediate one – P11) became projected wrongly (as from the inner zone). This ratio was very satisfactory although it must be remembered that PCA is not a classification technique by itself.

3.3.2. Procrustes rotation

A comparison of the PCA subspaces derived from each ría alone was made using Procrustes rotation. Consensus vectors were calculated by averaging out the PCs from both rías. These, together with the angles they form, can be seen in Table 5, where from it was observed that the angles that form the 1st PCs of each ría with the first consensus vector are small, ca. 1.4°, and so the first consensus vector (B1) resumed very well the main pattern of the samples on each ría. This consists of a general participation of all the variables, mainly of Cd and Hg, which ordered the samples in accordance with their total metallic content. This had also been seen in the 1st PCs of the studies above, as least polluted samples lie at the left hand side of Fig. 4. The second consensus vector was determined by Ni, which also happened for the independent PCAs of ROP and ROV. Nevertheless, small differences between the rías existed as the angle is a bit higher than for the 1st consensus vector (ca. 19°).

Table 4
Classification rules derived from some of the chemometric techniques (the figures correspond to concentration levels).

		PCA			CART		LDA[a]			SOM	
		Cd	Ni	Hg	Ni	Hg	DF1	DF2	DF3	Lowest	Highest
ROP	Outer-intermediate	≤0.20	<18	–	<23.3	<0.215	3.070	−1.633	−0.074	%TOC < 3 Zn < 150 Ni < 25 Pb < 50	
	Inner	>0.20	–	>0.7	<34.25	≥0.215	3.856	2.407	0.093		%TOC > 2 Cd > 0.2 Hg > 0.3
ROV	Outer	≤0.20	>25	–	<34.25≥23.3	<0.215	−1.141	−0.682	−1.564	%TOC < 3Cd < 0.2Cu < 3.5%TOC < 3.5	
	Intermediate	>0.20	>38	–	≥34.25	–	−3.441	0.509	−0.559		Zn > 150 Cu > 35 Ni > 25
	Inner	>0.20	>12<37	–	<34.25	≥0.215	−2.123	−0.349	2.774		%TOC > 3.5Zn (130–175)Pb > 100

[a] LDA centroids of autoscaled data.

Table 5
Consensus vectors and angles formed by the consensus vectors and the corresponding PCs obtained when comparing the two rías (autoscaled data).

	B1	B2
Consensus vectors		
%TOC	−0.40	0.23
Cd	−0.43	0.29
Zn	−0.37	−0.36
Cu	−0.37	−0.16
Hg	−0.42	0.09
Ni	−0.24	−0.77
Pb	−0.40	0.33
Angles		
ROV	1.41	19.33
ROP	1.41	19.33

3.3.3. *Hierarchical clustering and CART*

To complement the PCA studies, a hierarchical clustering analysis was made using the Euclidean distance and the Ward's grouping method. The heatmap clusters the samples and the variables and represents by tokens the (autoscaled) datum associated to a particular sample and a given variable. The scale at the left of Fig. 7 yields a self-explanatory graphical display of the data which allows for a fast interpretation of the groups.

The heatmap in Fig. 7 showed two main groups of samples, corresponding to the inner and intermediate (cluster C1) and the external (cluster C2) zones of the rías. They were subdivided further and some details are given below. Cluster C1-1 combined the samples with the overall highest concentrations of Hg, all them situated at ROP (surrounding the island of Tambo). This remarkable behaviour was justified because of its closeness to a chlorine–alkali industry and a paper pulp factory. In recent years severe actions were enforced to reduce mercury dumping into the ría of Pontevedra. Initially, they were quite successful and a decreasing trend was verified [50]. A recent increase was observed without a clear justification [51], although its origin may be related to historical undue waste water release into the ría, which would now yield some sort of 'cronic' level of Hg on the environment and, thus, affect the sediments.

Cluster C1-2 grouped the inner samples of ROV, which became characterized by the highest concentrations of Pb (see more details above). This group included also two samples from the intermediate region of ROV, V22 and V26, due to their high concentrations of Cu and Zn. Cluster C1-3 considers the remaining intermediate samples, along with an inner one (V30).

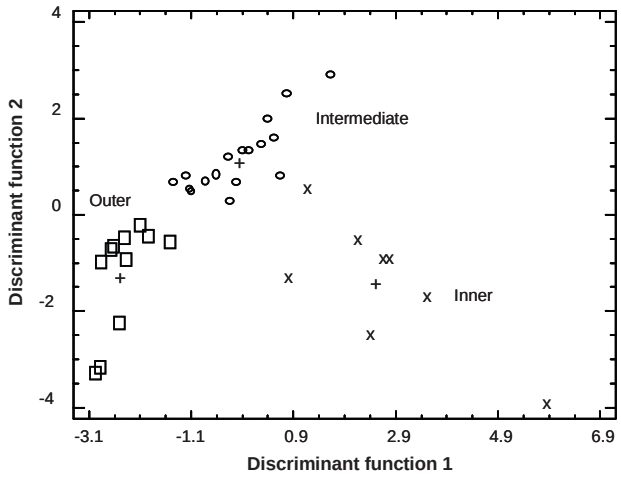

Fig. 9. Discriminant scores at the DF1-DF2 subspace calculated for the ría of Vigo. Codes: (□) outer-ROV, (○) intermediate-ROV, (×) inner-ROV, (+) centroids.

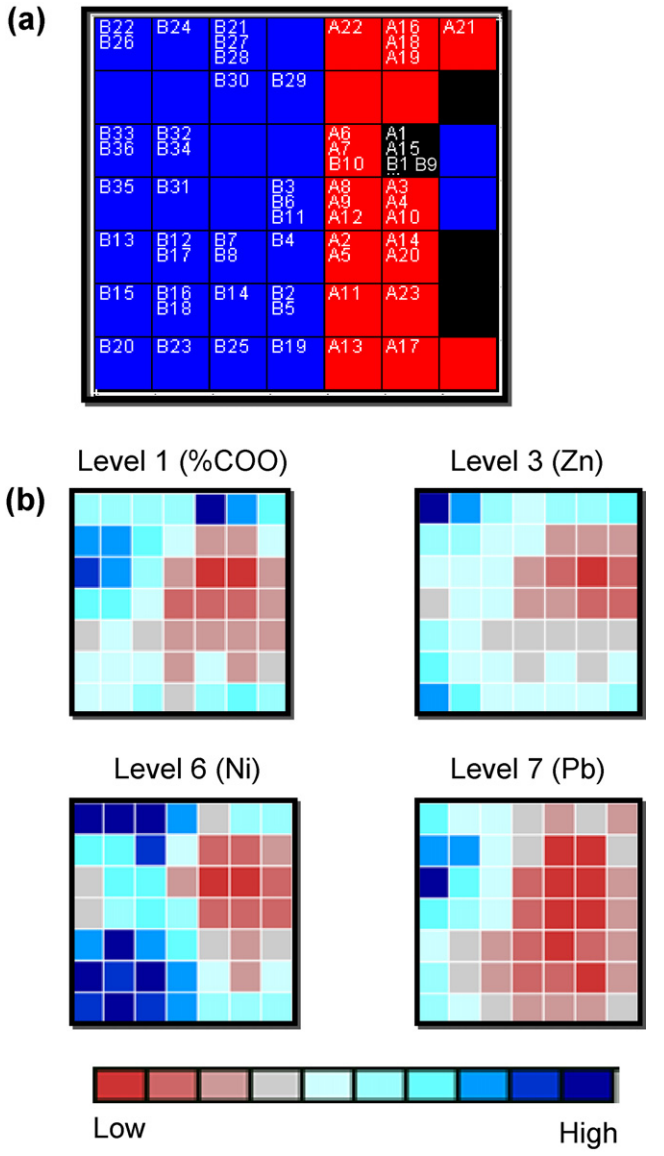

Fig. 10. Kohonen SOM differentiating the two rías. Top map (a) and relevant layers of weights characterizing the differences (b). Codes: A, ROP; B, ROV.

Cluster C2 joined the samples with the lowest figures in all metals and %TOC. They corresponded to the external zone of ROV and the external and intermediate ones from ROP. For instance, C2-1 contained those samples with the lowest concentrations in all metals, particularly Zn, Ni, and %TOC. They had been also observed at the left hand side in the PCA scores plot (see Fig. 4). C2-2 grouped the external samples from Vigo (all of them in a dedicated subgroup, from V2 to V6, Fig. 7) to a variety of samples from Pontevedra (external, intermediate and, even, inner, i.e. P14, P20 and P23). They had concentrations slightly higher than C2-1 but lower than those for the remaining samples.

CART seeks for a set of 'if . . . then' logical conditions that permit accurate classification of samples in a set of previously defined classes. Preliminary studies were made considering the outer and intermediate zones of ROP both altogether and separated (as their samples overlapped clearly in the PCAs). Results were not different and, thus, those in Table 4 corresponded to both zones considered altogether. Only two metals (Ni and Hg) were required to classify the sediments according to the rías and their morphological zones (Section 2.1). They yielded an 83% classification success. The intermediate ROV zones (along with two samples, each from the inner

and outer ROV zones) became defined by Ni concentrations ≥ 34.2. Values of Ni < 34.2 and Hg ≥ 0.215 leaded to a group of 17 samples, 10 corresponding to inner ROP and 7 from inner ROV (P13 to P 23, V 29 and V31 to V36, see Fig. 4). When Hg < 0.215 and 34.2 > Ni ≥ 23.3, the remaining outer ROV samples (V2 to V4, V6 to V8 and V11) became in a distinctive group. Finally, Hg < 0.215 and Ni < 23.3 described the outer and intermediate ROP sediments plus the three outer ROV samples (V1, V9 and V10, as expected after Fig. 4).

3.3.4. Linear discriminant analysis

A linear discriminant analysis (LDA) was made to differentiate the two rías and, likely, their morphological zones. Standardized data and the forward and backward procedures were employed (in both cases the same results were obtained). Accordingly, a discriminant function was calculated as $-2.20Zn + 0.90Cu - 0.64Hg + 1.68Ni + 1.01Pb$, with Zn and Ni being the most relevant metals giving rise to a good differentiation of the two rías. The centroids for ROV and ROP were +1.41 and −2.20, respectively. The contingency table showed a 94.92% success ratio and only three samples from ROV were misclassified as from ROP, as expected. They were the three V1, V9 and V10 samples studied above with small percentages of fine particles.

A LDA model was developed considering the same five groups of samples as those in the overall PCA above (Table 4). The forward procedure to introduce variables in the discriminant functions, DF, and the Wilks' lambda function to assess the significance of each DF were used. This yielded three significant DFs (99.99% explained variance) with three experimental variables on each (autoscaled data). The first function (73.52% explained variance) was associated to three heavy metals which appeared relevant also in the explanations of the PCA studies:

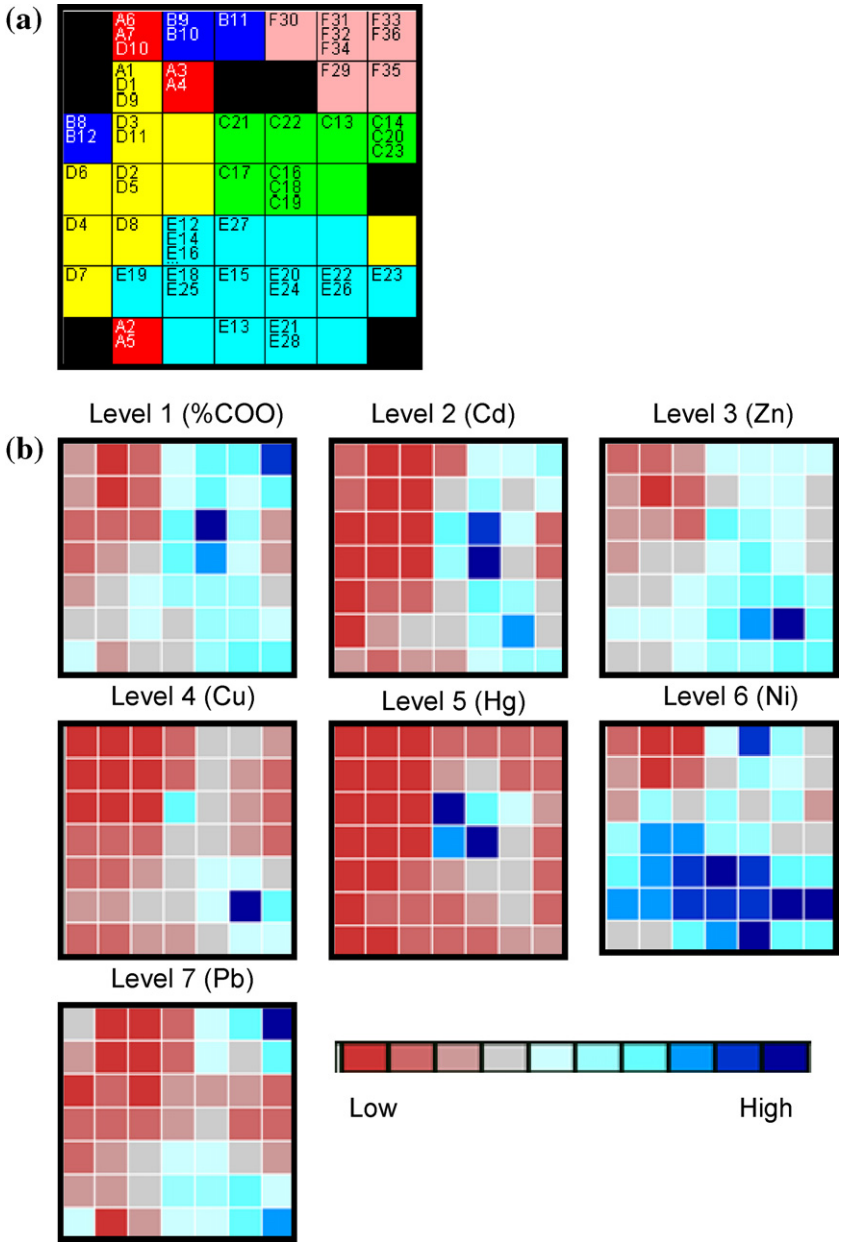

Fig. 11. Kohonen SOM differentiating the different areas within the two rías. Top map (a) and relevant layers of weights characterizing the differences (b). Codes: A, outer-ROP; B, intermediate-ROP; C, inner-ROP; D, outer-ROV; E, intermediate-ROV; F, inner-ROV.

+0.94Hg – 0.97Ni – 0.68Pb. The second DF (14.63%) was defined mostly by Hg: +0.87Hg + 0.25Ni – 0.04Pb, whereas the third function (11.84%) was linked to Pb: +0.05Hg –0.58Ni + 0.89Pb (in all cases these were standardized coefficients). Table 4 displays the centroids associated to each location, and a 87.93% classification success was obtained. Fig. 8 shows a good differentiation between the two rías, as well as between the three areas of ROV and the inner part of ROP.

Wrong classifications are explained briefly. P11 (intermediate ROP, was included as outer ROV because of its contents on Ni and Pb, higher than their ROP counterparts). Three inner samples from ROP: P14, P20 and P23 were classified as outer-intermediate because its concentrations on Hg, Ni and Pb were lower than the average value for the other inner samples. Three samples from ROV were assigned also to nearby groups: V19 (intermediate site considered as outer because it had concentrations of Ni and Pb lower than the average of the remaining intermediate samples); V29 (an inner sample classified as outer Vigo, without a clear explanation); and V30 (inner site considered as intermediate because the concentrations of Ni and Pb were higher and lower–respectively- than their counterparts, close to those of the intermediate samples).

Individual LDAs were made for each ría alone in order to differentiate each zone (external, intermediate and inner). Results for ROP were not good as a large overlap was obtained for the external and intermediate samples (as it had been observed in the studies above). This reflected the similarity between the samples of this ría, with high concentrations of metals both at the northern shore and the area 'protected' by the Ons Islands. Hence, LDA results for this ría will not be presented. On the contrary, a nice differentiation between the three ROV zones was obtained. This was justified by the clear impact that some anthropogenic activities caused in some particular points (city of Vigo, harbour of Vigo, an old pottery factory, etc.).

Two discriminant functions were calculated for ROV. The 1st, explained 70.3% of the variance and was defined as $+1.03 \times \%TOC + 0.25Hg - 0.51Ni$; the 2nd function (29.7% of the variance) was $-0.39 \times \%TOC + 0.58Hg + 0.87Ni$. Fig. 9 presents the ROV samples projected on the space of the two discriminant functions where the three zones can be separated quite clearly. The contingency table revealed a 97.22% overall classification success, with only a wrong sample (V30). This was considered intermediate due to its medium-high Ni concentration (37.0 mg kg^{-1}), compared to the average value of its inner counterparts (ca. 24.0 mg kg^{-1}). In Fig. 9 this corresponds to the cross which lies closer to the circles. The centroids of the classes are given in Table 4.

Fig. 9 shows that DF1 differentiates quite well the three zones because of TOC, which increases steadily when entering the ría (despite a slight overlap exists among the intermediate and inner zones). DF2 separates those two zones, but for sample V30, thanks to the differences in Ni (higher values at the intermediate region).

3.3.5. Self-organizing maps

Kohonen neural networks or SOMs were applied as an advanced unsupervised method to unravel classes [55]. Three situations will be considered, as in the previous techniques; namely, both rías altogether and each ría by separate.

A 7×7 square net, trained for 500 epochs and an initial learning span equivalent to a third of the neurons of the net, allowed a clear differentiation between the two rías (autoscaled data, Fig. 10a). As expected, samples V1, V9 and V10 (now renamed to B1, B9 and B10 due to software constraints) became in the SOM region that was attributed to the ría of Pontevedra. This was acceptable because they had very low concentrations of metals due to the very low percentages in fine particles, as discussed above. The neuron activated by V1 and V9 (renamed to B1 and B9) from ROV was not assigned to a specific group because it was activated also by two samples from ROP (renamed as A1 and A15).

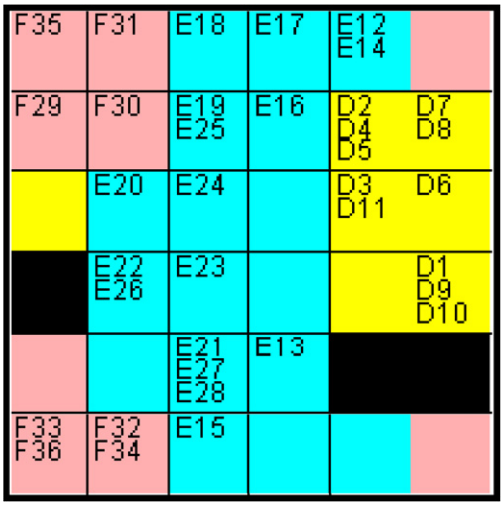

Fig. 12. Top map of the Kohonen SOM showing different areas within the ría of Vigo. Codes: D, outer-ROV; E, intermediate-ROV; F, inner-ROV.

The weights that determined the differentiation between the rías were, basically, those at level 1 (corresponding to %TOC, so that lowest weights – i.e., lowest percentages-corresponded to ROP), and levels 3, 6 and 7 (linked to Zn, Ni and Pb, respectively; with highest weights – i.e., concentrations-associated to ROV, see Fig. 10b).

An additional study was undergone to evaluate whether the six geographical zones could be observed in a SOM. The same architecture as that in the previous study was employed to develop a new SOM. Fig. 11a shows that four zones could be differentiated nicely although the external and intermediate zones of ROP mixed (as expected after the previous studies).

The layers that determined most the 'discrimination' between the groups are presented in Fig. 11b. The external and intermediate zones of ROP (codified by letters A and B, respectively) were characterized by lowest weights (concentrations) in %TOC, Cd, Zn, Cu, Ni and Pb. The internal zone of ROP (codified as C) got restricted to a reduced number of neurons (a tight group of samples) with highest weights for the layers associated to %TOC, Cd and, specially, Hg. The external area of ROV (codified as D) got characterized by low weights (experimental values) for %TOC, Cd and Cu, and also intermediate-low values for Zn. On the contrary, the intermediate zone of ROV (E codes) presented high weights for Zn, Cu and Ni and, also, medium values of %TOC. Finally, the inner part of ROV (F codes) became defined by high weights in the %TOC and Pb layers.

The three zones of ROV were studied further by a dedicated SOM (a 7×7 square net, trained for 300 epochs and an initial learning span equivalent to a third of the neurons of the net), which attained a satisfactory result as they three became very well differentiated (Fig. 12). The interpretation of the weights was straightforward and the figures are not presented for brevity. The external part of the ría (D codes) was characterized by low weights–concentrations- of Cd, Zn, Cu, Hg, Pb and %TOC. The intermediate area (E codes) was marked by high values on Zn, Cu, Hg and Ni. The inner zone of ROV could be defined by high values on Pb.

4. Conclusions

The spatial distribution of trace metals in the rías of Pontevedra and Vigo was closely related to the content of fine particles in the sediments and, accordingly, to the content of organic matter. The percentage of fine fraction and organic carbon was highly

dependent on artificial inputs, such as wastes of industrial activities, sewage effluents and aquaculture activities and, therefore, trace metals tend to accumulate in the fine fraction of the sediments close to these sources.

In general, the distribution of the trace metals was more homogeneous in ría of Pontevedra (where the inner and intermediate morphological zones could not be differentiated) than in ría of Vigo (where the three morphological zones were differentiated, according to TOC and/or Cd). Both rías can be differentiated quite well using a reduced set of two metals: Ni and Hg, as derived from CART. These metals were indeed relevant to define the most important factors extracted in PCA, LDA and Procrustes rotation. Hg was clearly linked to the industrial activities of the ría of Pontevedra while a definite origin could not be ascertained for Ni. In fact, it seems that Ni has a strong lithological origin at the ría of Vigo.

The joint pollution assessment revealed that both rías presented several degrees of pollution caused by different trace metals. Pollution levels in ROP were not as high as those observed in ROV, except for Hg, since 43.5% and 26.1% of samples in ROP overpass the ERL and ERM limits respectively. Nevertheless, for most metals, more than 65% of samples showed concentrations below the ERL. On the contrary, pollutant concentrations in ROV are quite high for all metals and, except for Cd, between 60% and 80% of sites surpass the different ERL values. Besides, 5.6% sampling sites went beyond the Pb ERM limit.

Acknowledgements

This study was financed by the Instituto Español de Oceanografía (IEO) and performed within its Marine Pollution Program. The authors thank the crew of the R/V José María Navaz and the technical staff for their contribution to the collection and preparation of the samples. Cristina Quelle thanks the 'Dirección Xeral de Investigación, Desenvolvemento e Innovación' of the 'Consellería de Innovación e Industria' for a 'Isabel Barreto' Grant, within the Human Resources Program of the 'Xunta de Galicia'.

References

[1] K.S. Kumar, K.S. Sajwan, J.P. Richardson, K. Kannan, Mar. Pollut. Bull. 56 (2008) 136.
[2] S.M. Rowlatt, ICES Coop. Res. Rep. 208 (1995).
[3] P.M. Chapman, F. Wang, Environ. Toxicol. Chem. 20 (2001) 3.
[4] M. Turkmen, A. Turkmen, Y. Tepe, A. Ates, K. Gokkus, Food Chem. 108 (2008) 794.
[5] A. Palaques, P. Puig, J. Guillén, X. Querol, A. Alastuey, Sci. Total Environ. 242 (1999) 211.
[6] G.A. Burton, Limnology 3 (2002) 65.
[7] D.J. McCauley, G.M. DeGraeve, T.K. Linton, Environ. Sci. Policy 3 (2000) 133.
[8] R. Hubner, K.B. Astin, R.J.H. Herbert, J. Environ. Monit. 11 (2009) 713.
[9] E.R. Long, D.D. MacDonald, S.L. Smith, F.D. Calder, J. Environ. Manage. 19 (1995) 81.
[10] K.D. Daskalakis, T.P. O'Connor, Mar. Environ. Res. 40 (1995) 381.
[11] A.G. Stevenson, Cont. Shelf Res. 21 (2001) 879.
[12] R. Beiras, J. Bellas, Aquaculture 277 (2008) 208.
[13] P. Sánchez-Marín, R. Beiras, Aquat. Living Resour. 21 (2008) 57.
[14] V. Besada, J.M. Andrade, F. Schultze, J.J. González, Ecotoxicol. Environ. Saf. 74 (2011) 373.
[15] V. Besada, J.M. Andrade, F. Schultze, J.J. González, Cont. Shelf Res. 31 (2011) 457.
[16] R. Prego, A. Cobelo-García, Environ. Pollut. 121 (2003) 425.
[17] P. Herbello, R. Prego, Ser. Quím. Oceanogr. 2 (1998) 1.
[18] A.J. Marmolejo-Rodríguez, A. Cobelo-García, R. Prego, Soil Sediment Contam. 16 (2007) 557.
[19] R. Prego, A.V. Filgueiras, J. Santos-Echeandía, Mar. Pollut. Bull. 56 (2008) 1031.
[20] J. Canario, R. Prego, C. Vale, V. Branco, Water Air Soil Pollut. 182 (2007) 21.
[21] F. Vilas, M.A. Nombela, E. Garcia-Gil, S. Garcia-Gil, I. Alejo, B. Rubio, O. Pazos (Eds.), Cartografía de Sedimentos Submarinos, C.d.P. Xunta de Galicia, Marisqueo e Acuicultura, Fundación Provigo, Universidad de Vigo, Ría de Vigo, E: 1:50.000, 1995.
[22] B. Rubio, M.A. Nombela, F. Vilas, Mar. Pollut. Bull. 40 (2000) 968.
[23] M. Álvarez-Guerra, D. Ballabio, J.M. Amigo, J.R. Viguri, R. Bro, J. Chemometr. 24 (2010) 379.
[24] W. Wooster, A. Bakun, D.R. McLain, J. Mar. Res. 34 (1976) 131.
[25] J.O. Blanton, L. Atkinson, F. Castillejo, A. Lavín, Rapp. P. Réun Cons. Int. Explor. Mer. 183 (1984) 79.
[26] A.F. Ríos, F.F. Pérez, X.A. Álvarez-Salgado, F.G. Figueiras, Deep Sea Res. 39 (1992) 645.
[27] R.A. Varela, G. Roson, J.L. Herrera, S. Torres-López, A. Fernández-Romero, J. Mar. Syst. 54 (2005) 97.
[28] D.W. Pritchard, Proc. Am. Soc. Civ. Eng. 81 (1955) 1.
[29] G. Roson, F.F. Perez, X.A. Álvarez-Salgado, F.G. Figueiras, Estuarine Coastal Shelf Sci. 41 (1995) 195.
[30] F. Ruíz, Mar. Pollut. Bull. 42 (2001) 482.
[31] V. Besada, F. Schultze, Mineralización de sedimentos marinos con microondas para la cuantificación de metales pesados, XIII Encontro Galego-Portugués de Química., Ilustre Colegio Oficial de Químicos de Galicia, Vigo, Pontevedra, 1999.
[32] O.A. EL-Rayis, Rapp. Comm. Int. Mer. Médit 29 (1985) 45.
[33] B. Rubio, K. Pye, J.E. Rae, D. Rey, Sedimentology 48 (2001) 1277.
[34] P. Álvarez-Iglesias, B. Rubio, M. Pérez-Arlucea, Estuarine Coastal Shelf Sci. 70 (2006) 507.
[35] P. Álvarez-Iglesias, El registro sedimentario reciente de la Ensenada de San Simón (Ría de Vigo, Noroeste de España): interacción entre procesos naturales y actividades antropogénicas, Departamento de Geociencias Marinas y Ordenación del Territorio, Universiadad de Vigo, Vigo, 2006.
[36] L. Bartolome, I. Tueros, E. Cortázar, J.C. Raposo, J. Sanz, O. Zuloaga, A. de Diego, N. Etxebarria, L.A. Fernández, J.M. Madariaga, Mar. Pollut. Bull. 52 (2006) 1111.
[37] R. Beiras, N. Fernández, J. Bellas, V. Besada, A. González-Quijano, T. Nunes, Chemosphere 52 (2003) 1209.
[38] R. Beiras, N. Fernandez, J.J. González, V. Besada, F. Schultze, Mar. Pollut. Bull. 44 (2002) 340.
[39] R. Prego, A. Cobelo-García, Rev. Acad. Galega Cienc. 21 (2002) 67.
[40] M.J. Belzunce, J.R. Bacon, R. Prego, M.J. Wilson, J.J. Environ, Sci. Health., Part A Environ. Sci. Eng. Toxic Hazard. Subst. Control 32 (1997) 1271.
[41] V. Besada, J. Fumega, B. Cambeiro, in: R. Prego, J.M. Fernández (Eds.), Procesos biogeoquímicos en sistemas costeros hispano-lusos, Excma. Diputación Provincial de Pontevedra, Pontevedra, 1997.
[42] R.J. Howarth, G. Evans, I.W. Croudace, A.B. Cundy, Sci. Total Environ. 340 (2005) 149.
[43] J.M. Andrade, M.P. Gómez-Carracedo, W. Krzanowski, M. Kubista, Chemom. Intell. Lab. Syst. 72 (2004) 123.
[44] L. Wilkinson, M. Friendly, Am. Stat. 63 (2009) 179.
[45] L. Breiman, J.H. Friedman, R.A. Olshen, C.J. Stone, Classification and Regression Trees, Chapman & Hall, New York, 1984.
[46] F. Questier, R. Put, D. Coomans, B. Walczak, Y.V. Heyden, Chemom. Intell. Lab. Syst. 76 (2005) 45.
[47] A.M. Martínez, A.C. Kak, IEEE Trans. Pattern Anal. Mach. Intell. 23 (2001) 228.
[48] T. Kohonen, Eng. Intell. Syst. Elect. Eng. Commun. 9 (2001) 179.
[49] A.M. Fonseca, J.L. Biscaya, J. Aires-De-Sousa, A.M. Lobo, Anal. Chim. Acta 556 (2006) 374.
[50] V. Besada, J. Fumega, A. Vaamonde, Sci. Total Environ. 288 (2002) 239.
[51] V. Besada, J.M. Andrade, F. Schultze, J. Fumega, B. Cambeiro, J.J. González, J. Mar. Sci. 72 (2008) 320.
[52] P. Álvarez-Iglesias, B. Quintana, B. Rubio, M. Pérez-Arlucea, J. Environ. Radioact. 98 (2007) 229.
[53] S. Larsson, B. Bergback, M. Eklund, U. Lohm, Environ. Rev. 7 (1999) 53.
[54] M. Barlattani, L. Ferrandi, G. Fiocchi, N. Portaro, L. Triolo, G. Zappa, G. Lorenzini, G.F. Soldatini, in: P. Editore (Ed.), Responses of Plants to Air Pollution: Biological and Economic Aspects, Pisa, Italy, 1995.
[55] M. Álvarez-Guerra, C. Gonzalez-Pinuela, A. Andres, B. Galán, J.R. Viguri, Environ. Int. 34 (2008) 782.